



3 | Bacteriology | Research Article

Edwardsiella ictaluri T3SS effector EseN is a phosphothreonine lyase that inactivates ERK1/2, p38, JNK, and PDK1 and modulates cell death in infected macrophages

Ranjan Koirala,¹ Chanida Fongsaran,¹ Tanisha Poston,¹ Matthew Rogge,² Bryan Rogers,¹ Ronald Thune,³ Lidiya Dubytska¹

AUTHOR AFFILIATIONS See affiliation list on p. 16.

ABSTRACT EseN is an Edwardsiella ictaluri type III secretion system effector with phosphothreonine lyase activity. In this work, we demonstrate that EseN inactivates p38 and c-Jun-N-terminal kinase (JNK) in infected head-kidney-derived macrophages (HKDMs). We have previously reported inactivation of extracellular-regulated kinase 1/2 (ERK1/2). Also, for the first time, we demonstrated that EseN is involved in the inactivation of 3-phosphoinositide-dependent kinase 1 (PDK1), which has not been previously demonstrated for any of the EseN homologs in other species. We also found that EseN significantly affected mRNA expression of IL-10, pro-apoptotic baxa, and p53, but had no significant effect on anti-apoptotic bcl2 or pro-apoptotic apoptotic peptidase activating factor 1. EseN is also involved in the inhibition of caspase-8 and caspase-3/7 but does not affect caspase-9 activity. Repression of apoptosis was further confirmed with flow cytometry using Alexa Fluor 647-labeled annexin V and propidium iodide. In addition, we found that the E. ictaluri T3SS is essential for the inhibition of IL-1β maturation, but EseN is not involved in this process. EseN did not affect cell pyroptosis, as indicated by the lack of EseN impact on the release of lactate dehydrogenase from infected HKDM. The transmission electron microscopy data also indicate that HKDM infected with WT or an eseN mutant died by apoptosis, while HKDM infected with the T3SS mutant more likely died by pyroptosis. Collectively, our results indicate that E. ictaluri EseN is involved in inactivation of ERK1/2, p38, JNK, and PDK1 signaling pathways that lead to modulation of cell death among infected HKDMs.

IMPORTANCE This work has global significance in the catfish industry, which provides food for increasing global populations. *E. ictaluri* is a leading cause of disease loss, and EseN is an important player in *E. ictaluri* virulence. The *E. ictaluri* T3SS effector EseN plays an essential role in establishing infection, but the specific role EseN plays is not well characterized. EseN belongs to a family of phosphothreonine lyase effectors that specifically target host mitogen activated protein kinase (MAPK) pathways important in regulating host responses to infection. No phosphothreonine lyase equivalents are known in eukaryotes, making this family of effectors an attractive target for indirect narrow-spectrum antibiotics. Targeting of major vault protein and PDK1 kinase by EseN has not been reported in EseN homologs in other pathogens and may indicate unique functions of *E. ictaluri* EseN. EseN targeting of PDK1 is particularly interesting in that it is linked to an extraordinarily diverse group of cellular functions.

KEYWORDS *Edwardsiella ictaluri*, type III secretion system, T3SS effectors, EseN, apoptosis, phosphothreonine lyase, MAPK, PDK1

Enteric septicemia of catfish is an economically important disease of farmed-raised channel catfish, *Ictalurus punctatus*, and is caused by the Gram-negative bacterial

Editor John M. Atack, Griffith University - Gold Coast Campus, Southport, Gold Coast, Australia

Address correspondence to Lidiya Dubytska, lidiya_dubytska@subr.edu.

The authors declare no conflict of interest.

See the funding table on p. 16.

Received 11 August 2023 Accepted 22 August 2023 Published 5 October 2023

Copyright © 2023 Koiralaa et al. This is an openaccess article distributed under the terms of the Creative Commons Attribution 4.0 International license.

Downloaded from https://journals.asm.org/journal/spectrum on 11 March 2024 by 2600:1700:a58:5270:1448:6640:10f7:5203

pathogen Edwardsiella ictaluri. In many Gram-negative pathogens, type III secretion systems (T3SS) are an important component of virulence (1). Previously, we reported that a T3SS is essential for E. ictaluri virulence and intracellular replication (2) and plays an important role in programmed cell death of host cells (3). T3SS serve to deliver effector proteins into eukaryotic cells (1). The T3SS effectors are a large and diverse group of virulence proteins that mimic eukaryotic proteins in structure and function and target a variety of eukaryotic physiological functions (4).

Many of these effector proteins are enzymes that chemically alter host proteins to interrupt or rewire host signaling pathways, thereby promoting bacterial survival and replication (5-7). The modifications to the signaling pathways by a subset of pathogen effectors differ from host modifications in their irreversibility (8-12). Phosphothreonine lyases are one example of such an enzyme that removes phosphate without hydrolysis and in a manner that is not reversible (8, 12, 13). For the MAPK signaling systems, such chemical transitions have significant impact on innate immune signaling. When MAPKs are involved in combating bacterial infections and activating the innate immune response, signal transfer and pathway activation are based on rapidly reversing cascades of phosphorylation and dephosphorylation. Irreversible dephosphorylation can prevent all further signal transmissions regardless of changes in conditions and leaves cells vulnerable or defenseless to infection (9, 11, 14).

Recently, the substrate requirements for several phospholyases have been reported (15). For example, Shigella flexneri T3SS effector, OspF, can interfere with many host processes simultaneously, while Salmonella enterica SpvC is more specific for the MAPK activation loop. Each phospholyase may have its own preferred substrate and/or modify an array of substrates in host cells (15). Earlier, we demonstrated that E. ictaluri effector protein EseN belongs to a family of T3SS effector proteins with phosphothreonine lyase activity that inactivates extracellular-regulated kinase 1/2 (ERK1/2) (16). We have also demonstrated that EseN is involved in inhibition of the M1 phenotype of head-kidneyderived macrophages (HKDMs) in response to E. ictaluri infection (17) and is involved in modulation of pathways that control the immune response to infection and expression of transcription factors NF-κβ (c-rel and relB), creb3L4, socs6, and foxo3a (17). We have also demonstrated that E. ictaluri effector EseN interacts with the major vault protein (MVP) that can serve as a signaling scaffold for selecting specific MAPKs for inactivation during E. ictaluri infection (16, 18).

In this work, we demonstrated that E. ictaluri EseN, similar to its homologs Shigella OspF and Salmonella SpvC, can inactivate p38 and c-Jun-N-terminal kinase (JNK) MAPKs. Moreover, for the first time, we demonstrated that EseN is involved in inactivation of 3-phosphoinositide-dependent kinase 1 (PDK1) in phorbol-12-myristate 13-acetate (PMA) pretreated HKDM, a feature that has not been demonstrated in other EseN homologs. PDK1 is a serine/threonine-protein kinase that belongs to the AGC kinase family and plays a central role in regulating cell growth, survival, and proliferation (19). Inactivation of PDK1 within infected HKDM may demonstrate a unique mechanism by which EseN effects host cell responses. To further develop the model for E. ictaluri pathogenesis, we also investigated the involvement of EseN in regulation of programmed cell death by direct measurement of apoptotic caspase-3/7, caspase-8, and caspase-9 activities and quantifying apoptotic cells by flow cytometry using Alexa Fluor 647-labeled annexin V (AnnV) and propidium iodide (Prl). We also analyzed mRNA expression of several genes that play important roles in activation or inhibition of apoptosis, including apoptotic peptidase activating factor 1 (apaf1) (20), p53 (21), and baxa (22). Becasue IL-10 can correlate with apoptosis (23), IL-10 mRNA expression was also analysed. To examine the involvment of EseN in pyroptosis, we investigated IL-1B maturation and measured cytotoxicity through the detection of lactate dehydrogenase (LDH) release by infected HKDM.

Downloaded from https://journals.asm.org/journal/spectrum on 11 March 2024 by 2600:1700:a58:5270:1448:6640:10f7:5203.

RESULTS

EseN dephosphorylates pp38 and pJNK ex vivo

PMA does not significantly stimulate activation of p38 and JNK in uninfected HKDM (Fig. 1A and B; compare HKDM+ to HKDM–). In contrast, anisomycin, which is a specific activator of p38 and JNK (24), significantly stimulates activation of p38 and JNK in uninfected HKDM (Fig. 1C and D; compare HKDM + to HKDM–). Levels of pp38 and pJNK in PMA or anisomycin-stimulated HKDM were significantly reduced when HKDMs were infected with wild type (WT) and $\Delta eseN$ complement ($\Delta eseN/eseN$) compared to HKDM infected with $\Delta eseN$ (Fig. 1). These results indicate that EseN inactivates pp38 and pJNK during E. ictaluri infection.

EseN interacts with PDK1 in Y2H assay

Previously, we described the cloning of an EseN "bait" into pDEST32 and the making of a HDKM complementary DNA (cDNA) library in pDONR22 to act as "prey" in this Y2H system (16). Successful association of proteins in this assay is indicated by the expression of URA3 and HIS3 (two of three reporters) and the ability of the colony to grow without supplemented uracil and histidine, respectively. In addition to MVP (16), we recovered one colony that grew poorly without the uracil but grew well on medium lacking histidine in the Y2H assay.

This clone was then re-screened on medium lacking histidine with different concentrations of competitive inhibitor of the reporter HIS3 gene: 3-amino-1,2,4-triazole (3-AT). The previously described pDONR22-MVP was used as a positive control for interaction, while an empty pDONR22 was a negative control. The clone grew on media lacking histidine and on media lacking histidine and containing 10- and 25-mM 3-AT but not 50-mM 3-AT, indicating a moderate interaction between EseN and the cloned protein. This clone was also URA3-positive and sensitive to 0.2% 5-fluoroorotic acid, which is converted by URA3 to fluorodeoxyuridine, a toxic analog of uracil.

The pDONR22 from this clone was then purifide and sequenced. Based on a BLAST of the insert sequence, pDONR22 contained a 95% pdk1 cDNA. To confirm interaction, pDEST23-PDK1 and pDONR22-EseN were retransformed into the host, *Saccharomyces cerevisiae* strain MaV203. Activation of the reporter genes following transformation and quantitation of beta-galactosidase activity using o-nitrophenyl- β -D-galactopyranoside and chlorophenol red- β -D-galactopyranoside once again confirmed the interaction of EseN and PDK1 (Fig. 2).

EseN dephosphorylates pPDK1 ex vivo

To test if EseN is involved in inactivation of PDK1, we performed Western blot analyses of uninfected HKDM and HKDM infected with *E. ictaluri* WT, $\Delta eseN$, and $\Delta eseN/eseN$. PMA significantly (by t-test) stimulated PDK1 activation in uninfected HKDMs (Fig. 3A; compare HKDM+ to HKDM—). Dephosphorylated PDK1 was detected in the PMA-treated HKDM (Fig. 3) but was not detected in anisomycin-treated HKDM or untreated HKDMs. This observation is consistent with the fact that PMA can activate phosphoinositide 3-kinase (PI3K) (25) and lead to PDK1 activation, while anisomycin is a specific activator of p38 and JNK and does not affect PDK1 activation. Importantly, levels of pPDK1 in PMA-stimulated HKDM infected with WT and $\Delta eseN/eseN$ were significantly reduced compared to cells infected with $\Delta eseN$ (Fig. 3A and B). These results indicate that EseN is involved in pPDK1 dephosphorylation during *E. ictaluri* infection.

EseN modulates expression of genes involved in cell death

Because MAPKs and PDK1-AKT pathways are involved in regulation of cell survival and death, we studied the role of EseN in those processes. We analyzed mRNA expression of several genes that play important roles in activation or inhibition of apoptosis (Fig. 4), including anti-apoptotic *bcl2* (26), *apaf1*, a key indicator of apoptosis in the intrinsic

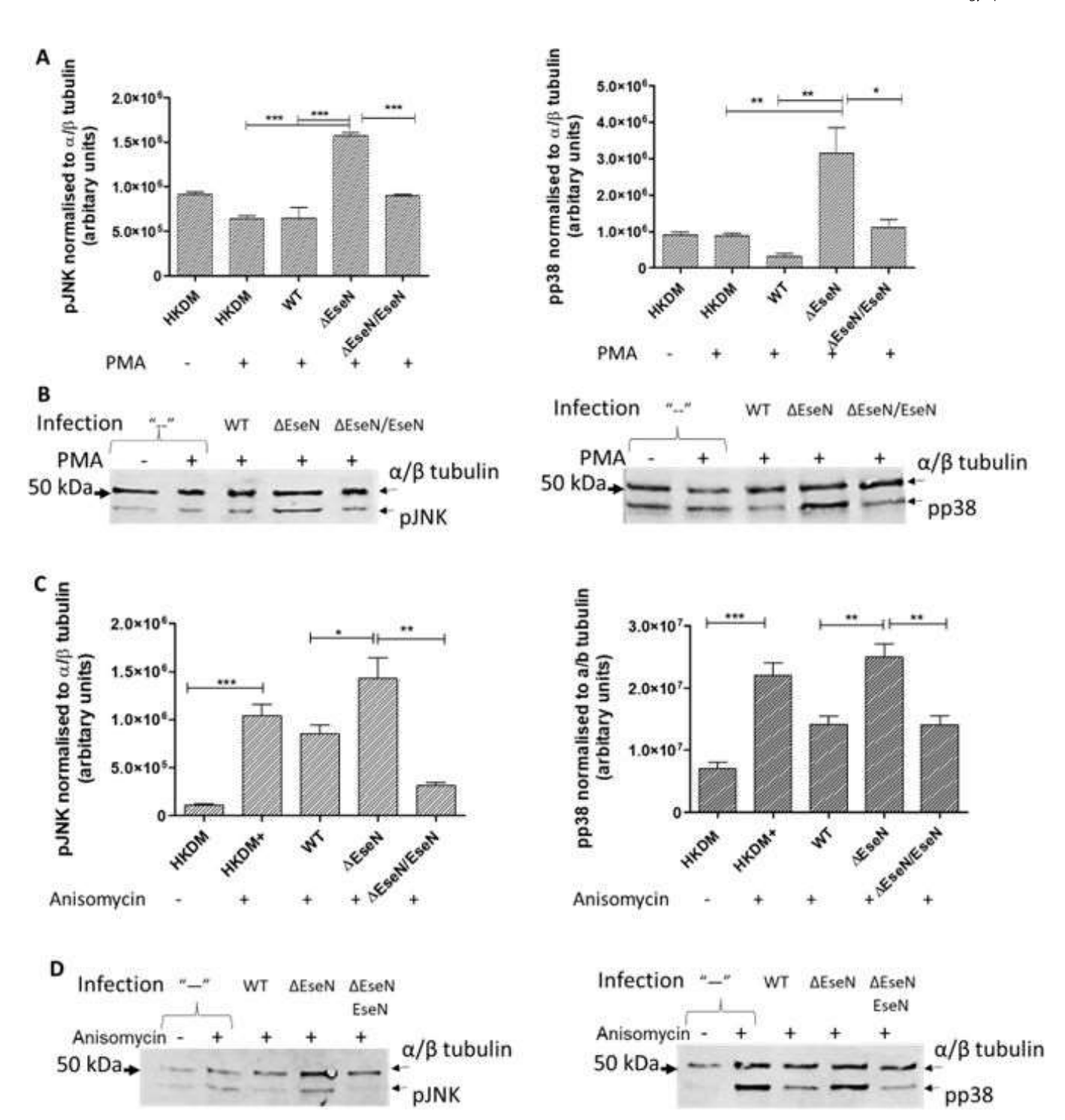


FIG 1 Western blot results showing inactivation of JNK and p38 ex vivo. (A and C) Levels of activation by phosphorylation of p38 and JNK detected in panels B and D, except quantified using a ChemiDoc MP imaging System (Bio-Rad) with bands normalized to α/β-tubulin. Comparison between groups was based on one-way analysis of variance with Tukey's post hoc procedure for comparison of group means. Mean \pm SD, N = 4-5, depending on treatment. Panels B and D show representative experiments that detect phosphorylated JNK and p38, ex vivo in uninfected channel catfish head-kidney-derived macrophages (HKDMs) infected with wild-type (WT) Edwardsiella ictaluri, mutant EseN (ΔeseN), or the ΔeseN complemented strain (ΔeseN/eseN) following stimulation for 15 min with phorbol-12-myristate 13-acetate (PMA) (B) or anisomycin (D). Both WT and the ΔeseN/eseN complemented strain inactivated p38 and JNK in HKDM stimulated with PMA (A and B) and anisomycin (C and D). *P < 0.05; **P < 0.01; ***P < 0.001.

pathway (20), pro-apoptotic gene *baxa* (22), and *p53*, which plays a role in controlling cell division and cell death (21). Levels of mRNAs were measured at 1, 3, 5, and 7 h

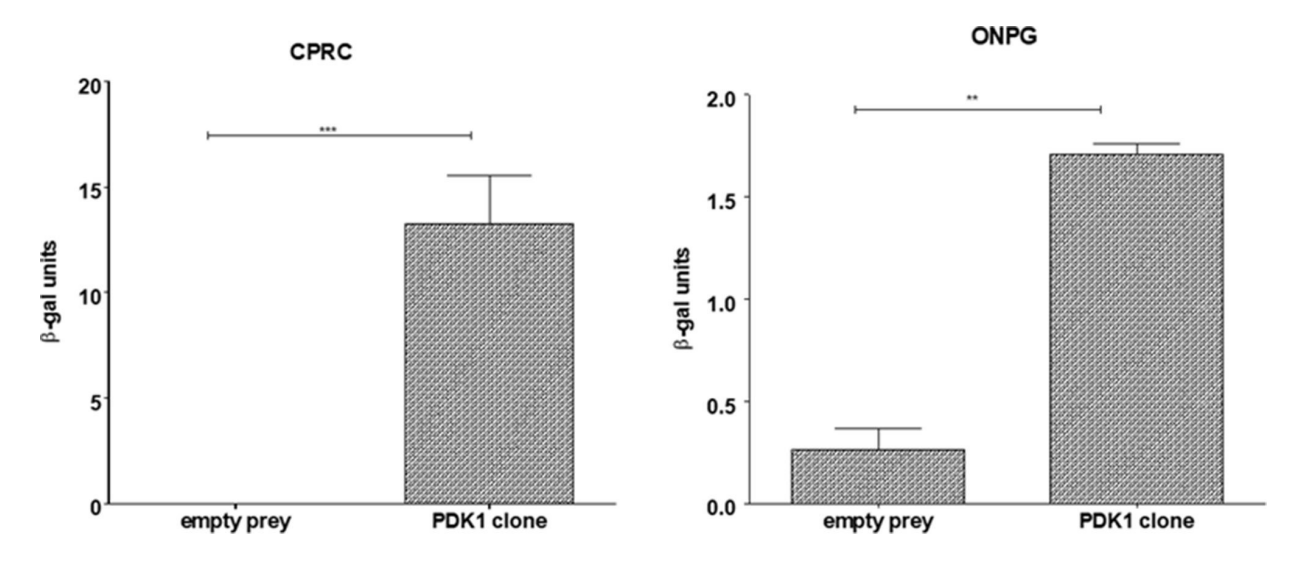


FIG 2 Quantitative assays for β-galactosidase (β-gal) activity for PDK1 clone in liquid culture using chlorophenol red-β-D-galactopyranoside (CPRG) or o-nitrophenyl-β-D-galactopyranoside (ONPG) as substrate. As a substrate, CPRG is more sensitive and the reaction time is faster than ONPG, but the strength of the reaction indicates the relative strength of the bait/prey interaction in both cases. Statistical analysis was conducted using t-test. Data are mean \pm SD of three replicates. **P < 0.01, **P < 0.001.

post-infection (PI) in uninfected HKDMs and HKDMs infected with WT and *E. ictaluri* $\Delta eseN$ by reverse transcription quantitative real-time PCR (RT-qPCR).

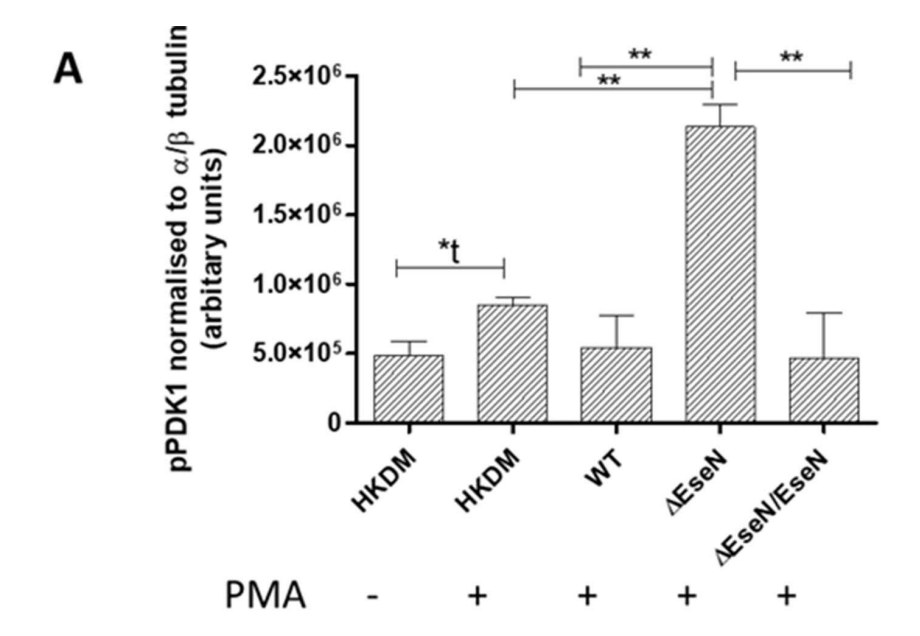
We did not detect significant differences in mRNA expression of anti-apoptotic bcl2 among HKDMs infected with any strains or at any time of infection (Fig. 4, top left). Results with apaf1 were similar to bcl2 except that the apaf1 mRNA expression ratio in HKDMs infected with $\Delta eseN$ was significantly higher at 7 h compared to 5 h PI (Fig. 4, top right). In contrast, EseN significantly affected mRNA expression compared to the two other tested pro-apoptotic genes. The mRNA levels were significantly upregulated in HKDMs infected with $\Delta eseN$ compared to WT at 3 h of infection for baxa and at 7 h of infection for p53 (Fig. 4, bottom left and bottom right).

It was reported that expression of IL-10 correlates with apoptosis (23) in infected HKDM. Therefore, we investigated IL-10 mRNA expression in HKDMs infected with WT and $\Delta eseN$ using uninfected HKDMs as a negative control. Infection with $\Delta eseN$ induced IL-10 production at 3 h PI compared to infection with WT at 3 h PI (Fig. 5). During 1, 5, and 7 h PI, no significant differences in IL-10 mRNA expression were detected between HKDM infected with WT or $\Delta eseN$. Collectively, these data indicate that during E. IL-10 infection, EseN is required for inhibition of IL-10 mRNA expressions that inhibit apoptosis in infected HKDMs.

Relationship between EseN and HKDM apoptosis

Caspase-8 activity in $\triangle eseN$ -infected HKDM was elevated at 1 and 3 h post-infection (Fig. 6) and did not differ at 7 h PI (Fig. 6, top row). Caspase-9 activity in WT-infected cells was lower than in $\triangle eseN$ -infected cells at 3 h PI only, but this difference was not significant (Fig. 6, middle row). Caspase-3/7 activity increased significantly in the $\triangle eseN$ -infected HKDM compared to WT-infected cells after 3 h PI but then declined to a WT level at 5 h PI. These data indicate that EseN is involved in inhibition of early apoptotic caspase-8 and suicide caspase-3/7 in infected HKDMs.

The relationship between EseN and macrophage apoptosis was further investigated by assessing the surface expression of phosphatidylserine using Alexa Fluor 647-labeled AnnV in conjunction with PrI after 5 h PI (Fig. 7). Early apoptotic cells bind annexin V, a Ca²⁺-dependent phospholipid-binding protein with a high affinity for externalized phosphatidylserine. Propidium iodide stains double-stranded DNA in cells with damaged cell membranes but fails to penetrate and stain cells with intact membranes. As shown



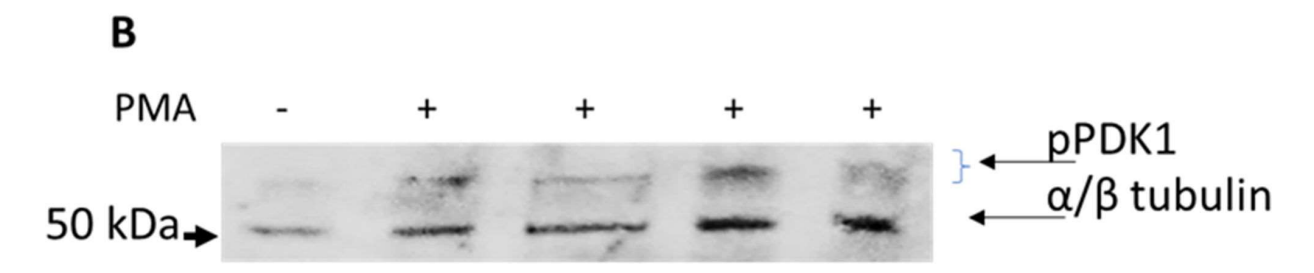


FIG 3 Western blot results of PDK1 inactivation. (A) Levels of activated pPDK1 as detected in panel B, quantified using a ChemiDoc MP imaging System (Bio-Rad) with bands normalized to α/β -tubulin. Comparison between groups was based on one-way analysis of variance with Tukey's post hoc procedure for comparison of group means. Mean \pm SD, N = 4-5, depending on treatment. (B) Result of a representative experiment detecting phosphorylated PDK1, *ex vivo* in uninfected channel catfish head-kidney-derived macrophages (HKDMs) infected for 15 min with wild-type (WT) *Edwardsiella ictaluri*, mutant *eseN* (Δ*eseN*), or the Δ*eseN* complemented strain (Δ*eseN/eseN*) following stimulation with phorbol-12-myristate 13-acetate (PMA). Both WT and the Δ*eseN/eseN* complemented strain inactivate PDK1 in HKDM stimulated with PMA. * $P \le 0.05$, ** $P \le 0.01$.

in Fig. 7, 37.89% of WT-infected HKDM cells and 31.37% of $\Delta eseN$ -infected HKDM were viable (AnnV–/Prl–). In addition, 23.49% of WT-infected cells were early apoptotic (AnnV+/Prl–), and 17.13% were late apoptotic (Ann+/Prl+), for a total of 40.63% positive for apoptosis. In contrast, infections with $\Delta eseN$ resulted in a significant increase in the level of early apoptotic cells at 32.27% but no significant increase in late apoptotic cells at 18.19% of total cells, for a total of 50.46% positive for apoptosis.

IL-1β activation during E. ictaluri infection of HKDM

To investigate if T3SS effector EseN can trigger macrophage cell death by inflammation, we evaluated IL-1 β release and maturation. Western blot analysis showed that *E. ictaluri* infection activates IL-1 β expression in infected HKDM (Fig. 8A). Differences between uninfected HKDM and HKDM infected with $\Delta eseN$ or T3SS mutant 65ST (2) were significant (P < 0.01) by non-parametric Kruskal-Wallis test and not significant by one-way analysis of variance (ANOVA) (Fig. 8A). Maturation of pro-IL-1 β to IL-1 β was detected in all infected HKDM independent of the bacterial strain (Fig. 8B and C). However, we did not detect any differences in IL-1 β maturation between HKDM infected with $\Delta eseN$ (Fig. 8B). Maturation of pro-IL-1 β to IL-1 β in

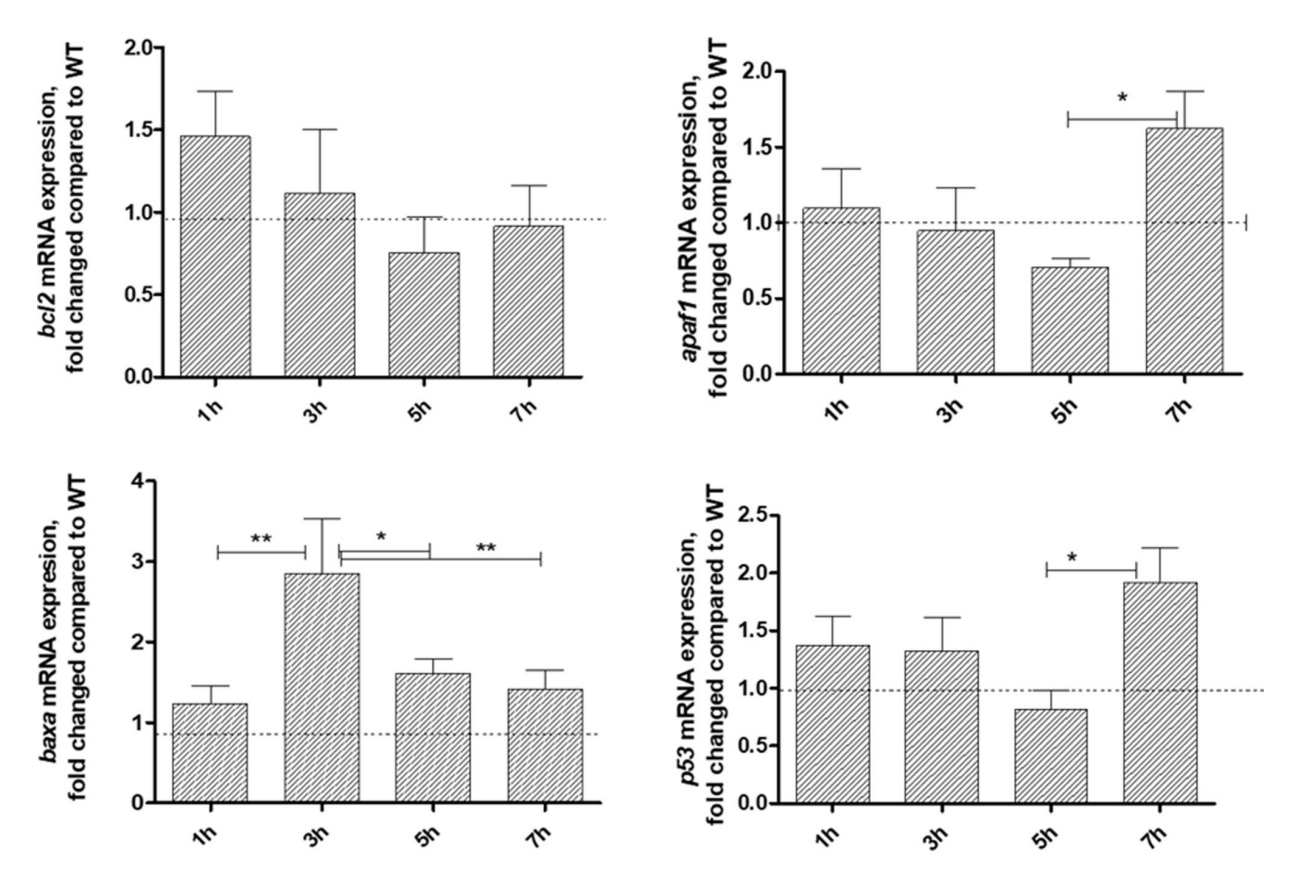


FIG 4 Fold changes of mRNAs expressed from HKDM infected with *E. ictaluri* $\Delta eseN$ compared to HKDM infected with *E. ictaluri* WT. Expression of mRNAs was measured by RT-qPCR at different time points post-infection. Data were collected and analyzed by Roche LightCycler 96 qPCR and software using relative expression method. *CanX* was used as the reference gene. Bars indicate fold changes in mRNA expression of HKDM infected with $\Delta eseN$ compared to WT. Fold changes were calculated after all data were normalized to the reference gene by dividing the mRNA expression in HKDM infected with $\Delta eseN$ by the number of mRNA expression in HKDM infected with WT. Results are presented as means and standard errors of the means and are combined data from four to five identical experiments, with three replications per treatment per experiment. *P \leq 0.05, **P \leq 0.01.

HKDM infected with 65ST was significantly higher than that in HKDM infected with WT or $\Delta eseN$, suggesting that other T3SS effectors are involved in inhibition of IL-1 β maturation.

Cellular damage in macrophages caused by invasion of E. ictaluri

To investigate if EseN plays any role in *E. ictaluri* cytotoxicity, we assessed membrane damage in HKDMs infected with WT or ΔeseN by measuring LDH release (Fig. 9) and examined cells with transmission electron microscopy (TEM) (Fig. 10C and D). There was no difference in cytotoxicity as shown by LDH release (Fig. 9) between HKDM infected with WT or ΔeseN. We also did not see membrane damage with EM (Fig. 10C and D).

Transmission electron microscopy of HKDM infected with E. ictaluri strains

TEM was used to visualize HKDM cell death in HKDM infected with WT, ΔeseN, and 65ST. Uninfected HKDM exhibited intact membrane and surface projections characteristic of healthy cells (Fig. 10A). Infection of HKDM with WT led to the formation of apoptotic bodies and nuclear shrinkage, but HKDMs maintained intact membranes (Fig. 10B). HKDM infected with ΔeseN demonstrated similar characteristics to HKDM infected with WT (Fig. 10C), except the number of cells forming apoptotic bodies was greater. Furthermore, in ΔeseN-infected HKDM, we detected nuclear fragmentation as well as apoptotic body formation. The HKDM infected with 65ST significantly differed from HKDM infected with WT and ΔeseN. Infection by 65ST caused formation of large vacuoles, many of which were surrounded by a double membrane which can indicate autophagy

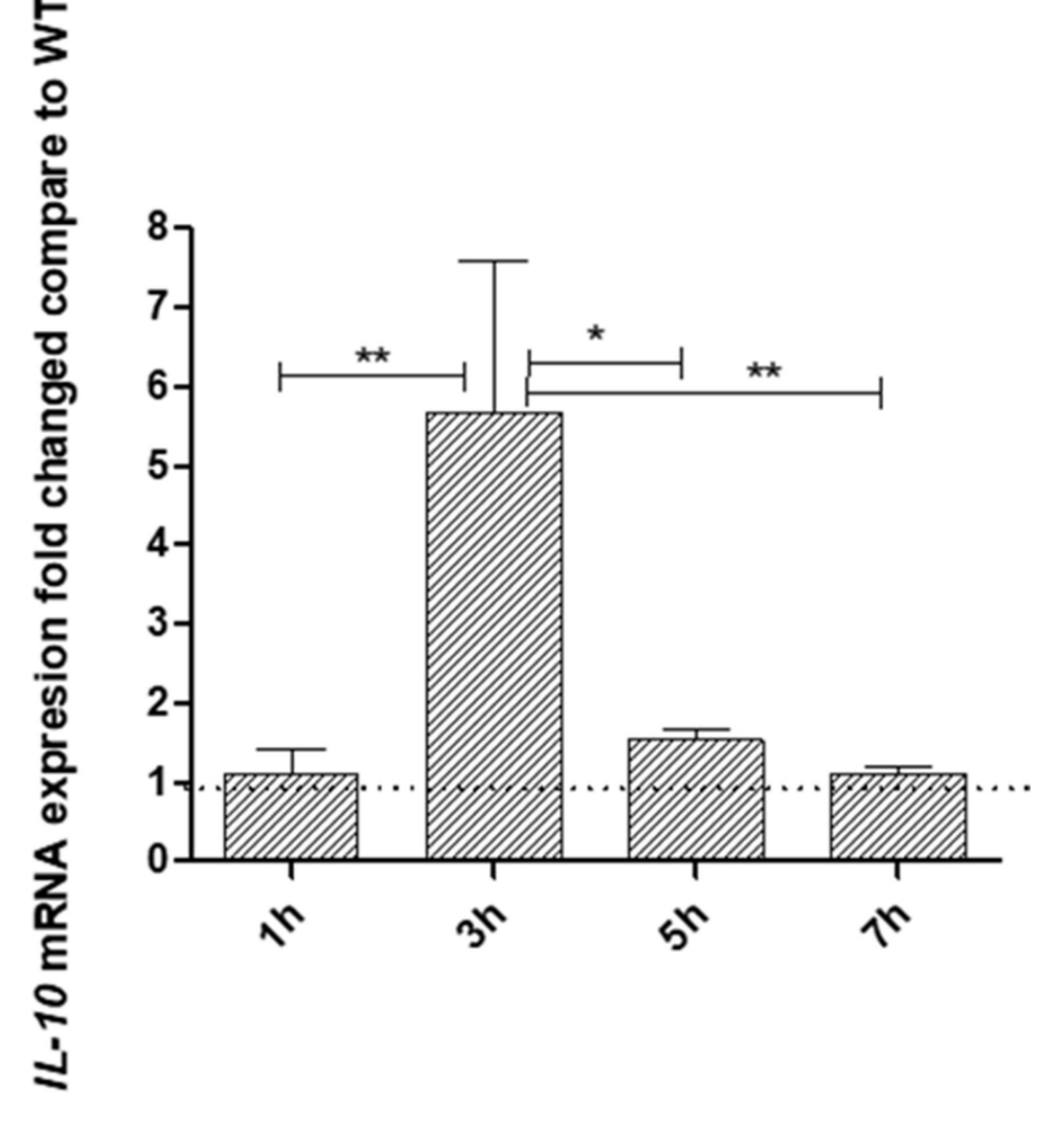


FIG 5 Fold changes of IL-10 mRNA expressed from HKDM infected with E. ictaluri AeseN compared to HKDM infected with E. ictaluri WT. expression of mRNAs was measured by RT-qPCR at different time points post-infection. Data were collected and analyzed by Roche LightCycler 96 qPCR and software using relative expression method. CanX was used as the reference gene. Bars indicate fold changes in mRNA expression of HKDM infected with ΔeseN compared to WT. Fold changes were calculated after all data were normalized to the reference gene and uninfected HKDMs by dividing the mRNA expression in HKDM infected with AeseN by the number of mRNA expression in HKDM infected with WT. Results are presented as means and standard errors of the means and are combined data from four to five identical experiments, with three replications per treatment per experiment. * $P \le 0.05$; ** $P \le 0.01$.

(Fig. 10D). Many cells also lost plasma membrane integrity, which correlates with our cytotoxicity study that was previously reported (3).

DISCUSSION

The E. ictaluri T3SS effector EseN belongs to a family of phosphothreonine lyases. EseN has 63% and 71% AA identity to the known T3SS effectors OspF in Shigella spp. and SpvC in Salmonella spp., respectively (27). Activation of MAPKs during WT infection leads to transcriptional reprogramming and induction of an innate immune response (28-31). However, subsequent dephosphorylation of pERK1/2 (16), pp38, and pJNK by EseN (Fig.

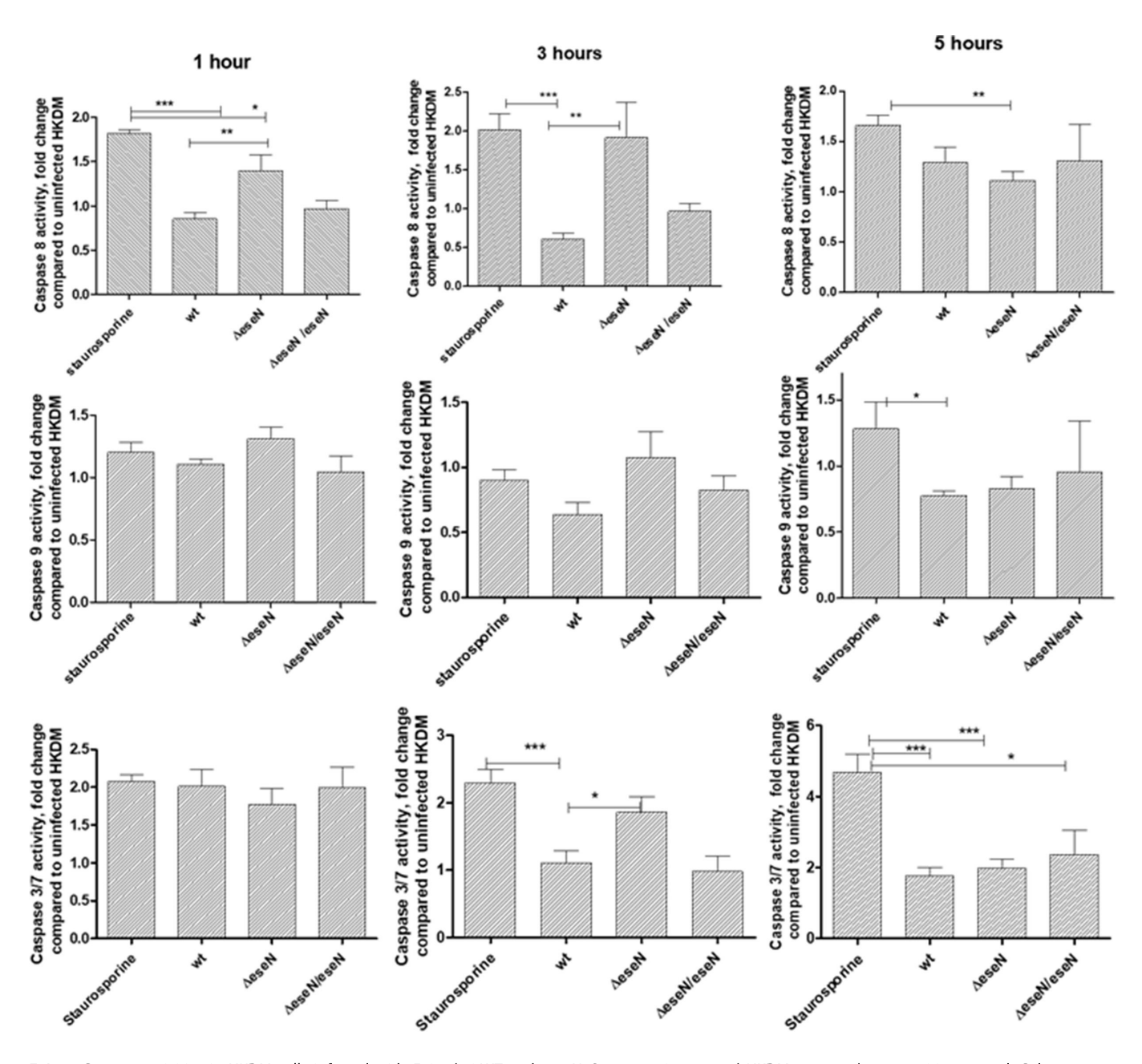


FIG 6 Caspase activities in HKDM cells infected with *E. ictaluri* WT and $\Delta eseN$. Staurosporine-treated HKDM was used as a positive control. Cultures were harvested at 1, 3, and 5 h post-infection. Values are expressed as means \pm standard deviation of four independent experiments. Asterisks indicate significant differences following one-way analysis of variance with Tukey's post hoc test to compare the mean of each treatment with every other treatment. Asterisks indicate significant difference between treatments. *P < 0.05, **P < 0.01, ***P < 0.001.

1) results in production of inactive ERK1/2, p38, and JNK, which downregulates the host inflammatory response (32, 33) and enhances proliferation of E. ictaluri (16). This is further supported by the reduction of the quantity of E. ictaluri in head-kidney following infection with the $\Delta eseN$ strain compared to the WT, as well as by a reduction in mortality (16). Interaction of EseN with the scaffold protein MVP (16) could regulate selection of MAPKs for dephosphorylation during the infection. Expression of EseN is enhanced during E. ictaluri invasion (34) of HDKM, which can lead to decreased phosphorylation levels of ERK1/2 (16), JNK, and p38. This MAPK inactivation results in the downregulation of the host immune response (17) and could at least be partially responsible for the death of infected HKDM.

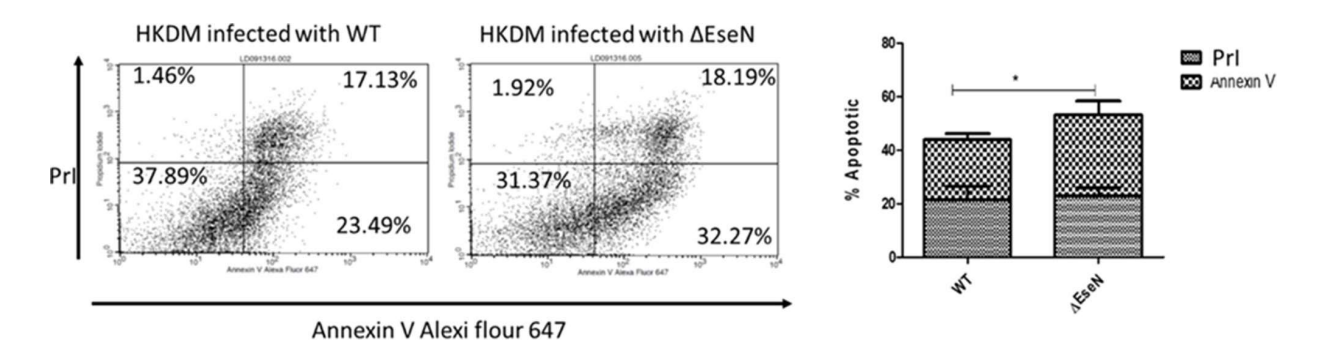


FIG 7 Assessment of HKDM by flow cytometry after annexin V/propidium iodide labeling. (A) Results are presented for one of three representative experiments. (Lower left) The percentage of cells that were viable (AnnV–/Prl–); (lower right) early apoptotic (AnnV+/Prl–); (upper right) late apoptotic (Ann+/Prl+). (B) Graph of the mean percentages of early and late apoptotic cells for the three experiments shows that the apoptotic HKDM infected with ΔEseN mutant was significantly greater than the WT. * $P \le 0.05$.

Interestingly, EseN is also involved in the dephosphorylation of PDK1 (Fig. 3). PDK1 activates downstream kinases, like Akt (35, 36), and has been shown to regulate protein synthesis, cell survival/death, glucose metabolism, and cell adhesion and migration. Multiple serine sites are phosphorylated on PDK1, and it has been demonstrated that serine 241 phosphorylation is required for PDK1 activity (35, 36). Tyrosine (Tyr-373/Tyr-376) phosphorylation may also regulate PDK1 activity (35, 36). Unfortunately, specific antibody to Tyr-373/Tyr-376 was not available for our study. Importantly, inactivation of PDK1 has not been demonstrated for any EseN homologs, indicating a possible unique function of this T3SS effector. Nevertheless, it was shown that *S. flexneri* effector OspF alters the phosphorylation of several hundred proteins, thereby demonstrating its broad impact during infection (37).

It was previously reported that MAPKs can be involved in regulation of programmed cell death (38–40). Cross-talk signaling between JNK, ERK1/2, and p38 MAPKs are important regulatory mechanisms in stress responses (41, 42). These kinases function in a cell context-specific and cell type-specific manner and integrate signals at different points through both transcriptional and post-translational mechanisms, which can result in caspase activation (38).

A diverse set of JNK and p38 MAPK substrates and transcription factors that are regulated by those MAPKs have been identified and validated (43–45). One of the best known transcription factors regulated by the JNK and p38 MAPK cascades in apoptosis

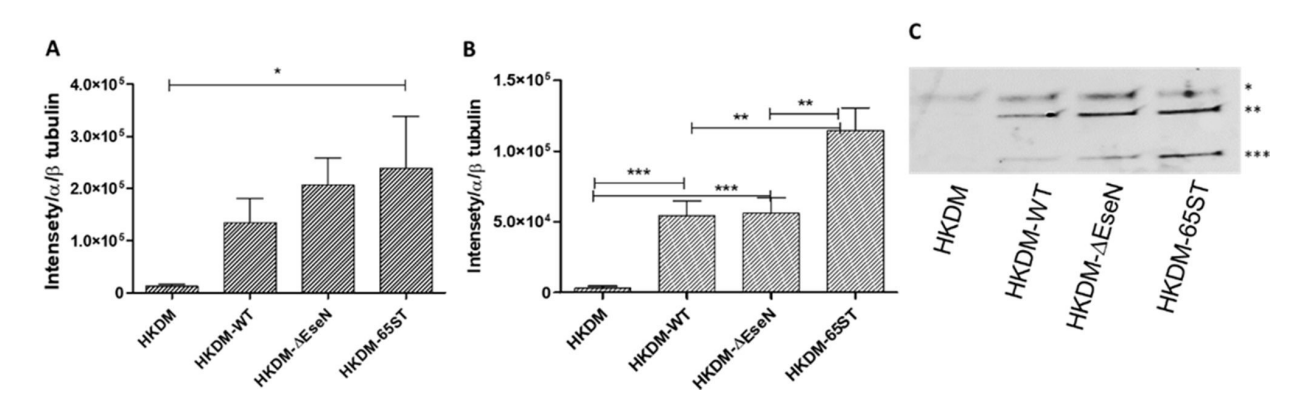


FIG 8 Inhibition of IL-1β maturation in HKDMs infected with *E. ictaluri*. (A and B) Graphical representation of pro-IL-1β (A) and IL-1β (B) expression in HKDM infected with either WT *E. ictaluri*, ΔeseN, or the T3SS mutant 65st based on the band intensities in Western blots from four independent experiments. Values are expressed as means ± standard deviation of four independent experiments. Asterisks indicate significant differences following one-way analysis of variance with Tukey's post hoc test to compare the mean of each treatment with every other treatment. Asterisks indicate significant difference between treatments. *P < 0.05, **P < 0.01, ***P < 0.001. (C) Representative Western blots that detected pro-IL-1β and IL-1β *ex vivo* in uninfected HKDMs, HKDM infected with wild-type (WT) *Edwardsiella ictaluri*, mutant EseN (ΔeseN), and 65ST. *, α/β-tubulin; ***, pro-IL-1β; ****, matured IL-1β.

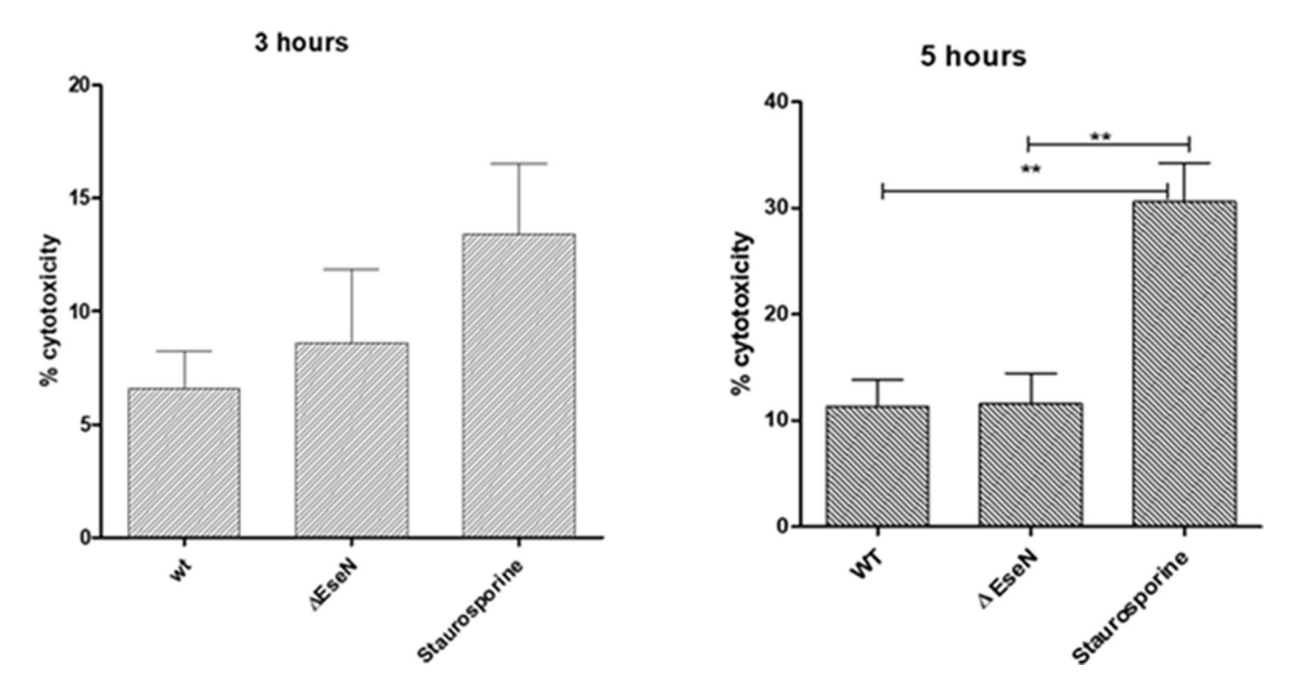


FIG 9 Release of LDH by HKDM infected with *E. ictaluri* WT and $\Delta eseN$. Cytotoxicty was based on release of LDH and detected using the CytoTox-ONE homogeneous cytotoxicity assay as described in Materials and Methods. Staurosporine-treated HKDM were used as a positive control. One-way analysis of variance with Tukey's post hoc test was used to compare the mean of each treatment with every other treatment. Asterisks indicate significant difference between treatments (N = 3).**P < 0.01.

is p53 tumor suppressor protein. In stressed cells, JNK-mediated phosphorylation can stabilize and activate p53 and thus promote programmed cell death (46) in combination

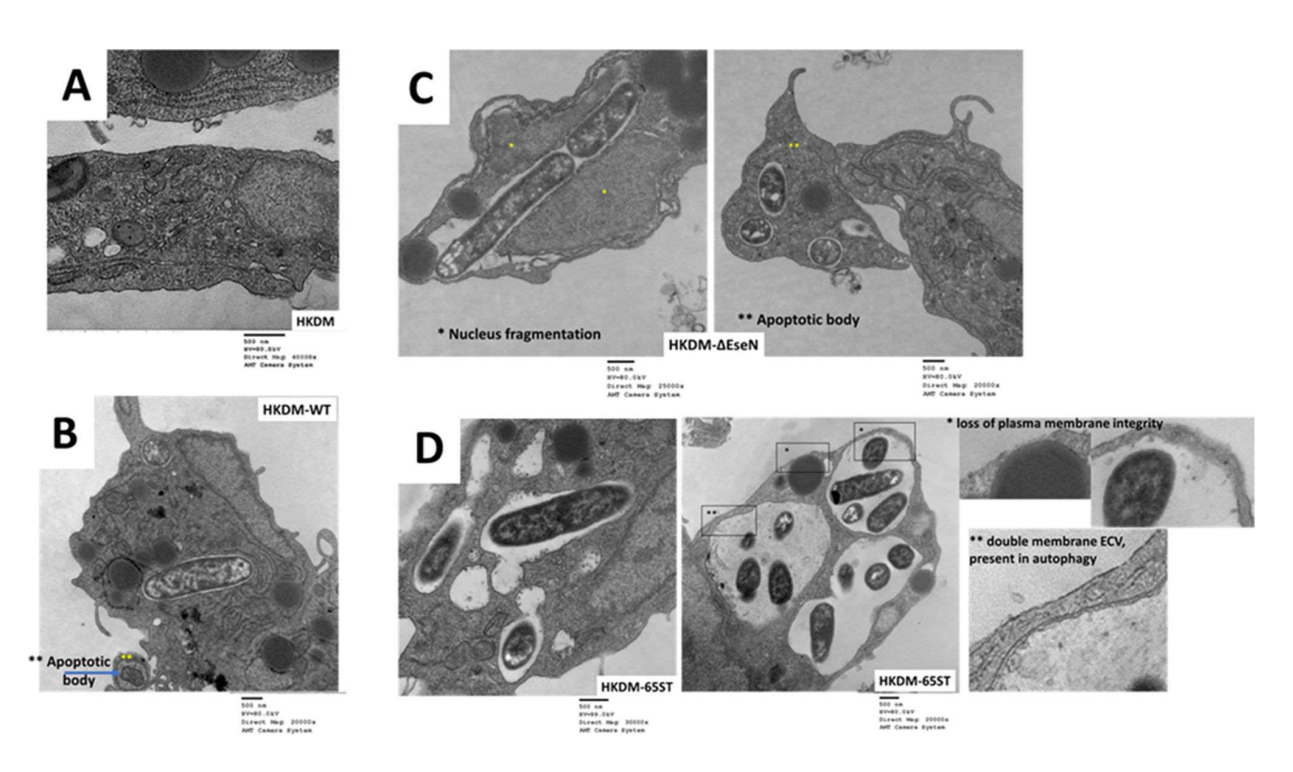


FIG 10 Transmission electron microscopy images of HKDM infected with different strains of *E. ictaluri*. (A) Uninfected HKDM showing normal structure and intact plasma membrane. (B) HKDM infected with WT showing intracellular *E. ictaluri* and apoptotic bodies (**). (C) HKDM infected with ΔeseN showing nuclear fragmentation (*) and apoptotic bodies (**). (D) HKDM infected with 65ST, showing large vacuoles containing *E. ictaluri*, double membranes (**, inset) typical of autophagy, and loss of plasma membrane integrity (*, inset). Infected cells were harvested 5 h PI, fixed, and prepared for TEM.

with other proteins. It was reported that p53-p73 dimerization is critical in the induction of apoptotic cell death, particularly as part of the JNK-mediated cell stress response. The p53-p73 dimer facilitates the expression of several pro-apoptotic target genes, such as *puma* and *bax* (47). Our data indicate that EseN was involved in regulation of *p53* mRNA expression in a time-dependent manner and was upregulated only at 7 h PI (Fig. 4). EseN also inhibits pro-apoptotic *bax* mRNA expression at 3 h PI but has no effect on anti-apoptotic *bcl*-2 mRNA expression. Yue and López reported that *bax* and *bcl*-2 are under the control of JNK and/or p38 MAPK cascades at a transcriptional and/or post-transcriptional level (38).

Previously, we reported that *E. ictaluri* T3SS effector EseN is involved in regulation of *foxo3a* mRNA expression in infected HKDM (17). FOXO3a mediates multiple physiological and pathological processes by inducing transcription of target genes involved in apoptosis (48, 49), proliferation (49), cell cycle progression (50), survival (51), and DNA damage (52). Together with current data, this demonstrates the importance of EseN in the modulation of HKDM apoptosis.

Interestingly, monocytes undergoing spontaneous apoptosis *in vitro* changed their cytokine production profile and are characterized by upregulation of IL-10 (23). These differences are seen both at the protein and mRNA levels and directly correlate with the appearance of apoptotic cells in the culture (23). *IL-10* mRNA was also upregulated in HKDM infected with the $\Delta eseN$ mutant at 3 h PI (Fig. 5), indicating that EseN is involved in the inhibition of pro-apoptotic *IL-10* mRNA production during this time.

Caspases play an important role in the initiation and activation of programmed cell death. Caspase-9 triggers intrinsic or mitochondrial signaling pathways of apoptosis, while caspase-8 triggers extrinsic or cell surface receptor pathways (53). Initiation of either of these pathways leads to activation of the executioner caspase-3 and caspase-7, which activate substrates that mediate the changes that characterize apoptotic cells. The significant and early inhibition of extrinsic initiator caspase-8 activity at 1 and 3 h PI in the WT-infected cells compared to the lack of inhibition by $\triangle eseN$ indicates that EseN acts to repress caspase-8 activity. This EseN activity would prevent initiation of apoptosis by infection with WT. The lack of differences between HKDM infected with E. ictaluri WT and \triangle eseN in intrinsic initiator caspase-9 activity (Fig. 6) indicates that EseN is not significantly involved in modulation of caspase-9 activity. Interestingly, executioner caspase-3/7 activity is significantly lower at 3 h post-infection for WT compared to ΔeseN, presumably because of the suppression of caspase-8 at 1 and 3 h PI by EseN. The WT, however, is not significantly different from $\Delta eseN$ after 5 h post-infection. The increase in caspase-8 at 5 h PI in the WT would account for the WT increase in caspase-3/7, suggesting that the suppressive effect of EseN ends and/or some other factor activates caspase-8 (Fig. 6).

Inflammasome activation is an important innate immune activity that regulates at least two host responses that are protective against infections: (i) secretion of the pro-inflammatory cytokines IL-1 β and IL-18 and (ii) induction of pyroptosis, a form of cell death that is triggered by inflammation. Production of IL-1 β and IL-18, as well as induction of pyroptosis in infected cells, is protective against many infectious agents (54). Activation of inflammasomes by *Yersinia pestis* depends on the T3SS early in the infection, but later, it is antagonized by the T3SS effector YopK (55, 56). Infection of HKDM with both WT and $\Delta eseN$ E. ictaluri induces production of pro-IL-1 β , but maturation of pro-IL-1 β into IL-1 β is inhibited. Infection with the total T3SS mutant 65ST, which does not induce any of the T3SS effectors, allowed maturation of pro-IL-1 β into II-1 β , indicating that E. ictaluri T3SS effectors other than EseN are involved in the suppression of this response (Fig. 8).

In summary, EseN is required for efficient replication of *E. ictaluri* in catfish HKDM and for maximum virulence in the catfish host (16), and our data help to explain this process. Specifically, our data demonstrate that EseN inactivates p38 and JNK MAPKs that play an immunosuppressive role and can lead to fish mortality. EseN also is involved in inhibition of apoptosis and prolongs HKDM survival, which prolongs *E. ictaluri* replication

Downloaded from https://journals.asm.org/journal/spectrum on 11 March 2024 by 2600:1700:a58:5270:1448:6640:10f7:5203.

in infected HKDM. Also, for the first time, we demonstrated that EseN is involved in the inactivation of PDK1. However, the role EseN plays in PDK1 inactivation and the biological consequences remain to be studied.

MATERIALS AND METHODS

Bacterial strains

Edwardsiella ictaluri WT strain 93–146, T3SS knockout mutant 65ST (2), and T3SS EseN effector mutant $\triangle eseN$ (34) were grown for 16–18 h at 28°C to an $OD_{600} = 1.8$ to 2.0 in porcine brain-heart infusion broth. All strains grown in broth were aerated on a Max Q4450 incubated shaker (Thermo Scientific, Marietta, OH, USA).

Infection procedure

Isolation of HKDM was performed as previously described (57). The HKDM cells were seeded in six-well plates for Western blotting, RNA isolation, and TEM, and in 24-well plates for caspase activity. For *E. ictaluri* infection, respective bacterial strains were opsonized for 30 min in normal autologous serum and added in duplicate (for RNA purification, cell lysate collection, and electron microscopy [EM]) or triplicate (for caspase activity and LDH release) wells with HKDM cultures at a multiplicity of infection (MOI) of 10 bacteria to 1 HKDM. Uninfected cells were used as a negative control. After infection, plates were centrifuged at $500 \times g$ for 5 min to synchronize contact of the bacteria with the adhered cell layer and were allowed to incubate for 30 min, after which $100 \mu g/mL$ gentamicin was added for 1 h at $28^{\circ}C$ to kill any remaining extracellular bacteria. Finally, wells were washed once with channel catfish RPMI (ctRPMI) (57), after which channel catfish macrophage media (57) containing a $1-\mu g/mL$ bacteriostatic dose of gentamicin was used to control the extracellular growth of any bacteria released from the cells during the experiment.

Ex vivo dephosphorylation assay

To evaluate subsequent dephosphorylation and inactivation of p38, JNK, and PDK1 by EseN, HKDMs were harvested and infected with WT, ΔEseN, or the ΔeseN/eseN complemented strains of E. ictaluri. The p38 and JNK pathways were activated after 5 h with the addition of 1 μg/mL of PMA or 20-μM anisomycin for 15 min. PMA is a specific activator of group A (α , βI , βII , and γ) and group B (δ , ϵ , η , and θ) protein kinase Cs that lead to transient activation of ERK1/2, p38, and JNK (58), while anisomycin is a specific activator of p38 and JNK (24). PMA also activates PI3K (25), which can lead to PDK1 activation. Uninfected, PMA/anycomycin-untreated cells served as negative controls, while uninfected, PMA/anisomycin-treated cells served as positive controls. After PMA/anisomycin treatment, cell lysates were collected in radioimmunoprecipitation assay (RIPA) buffer (Cell Signaling Technology) supplemented with phenylmethylsulfonyl fluoride (PMSF) (Thermo Scientific), Halt Protease Inhibitor Cocktail (Thermo Scientific), and PhosSTOP (Roche Diagnostic GmbH). Before loading into the gel, samples were mixed with 4x protein loading buffer (LI-COR, Lincoln, NE, USA) supplemented with 2-mercaptoethanol (Sigma-Aldrich, St. Louis, MO, USA), boiled for 5 min, separated on a PAGE gel, and transferred to a polyvinylidene difluoride membrane (PVDF), blocked with 2.5% skim milk. Blots were visualized with rabbit anti-pp38, anti-PJNK, or pPDK1 (Ser241) antibody (Cell Signaling Technology). Anti- α/β tubulin was used as a loading control.

Y2H assay

Y2H assay was performed as previously described (16). The ProQuest Two Hybrid System (Invitrogen, Carlsbad, CA, USA) was employed to identify the specific protein binding partner for T3SS effector EseN. The HKDM cDNA library was cloned into pDEST22 to serve as the prey. EseN fused in frame to the GAL4 BD was constructed on pDEST32 to serve

as the bait (16). The bait and prey plasmids were then transformed into *Saccharomyces cerevisiae* strain MaV203 and cultured on YPAD medium. Interaction between prey and bait was detected according to the manufacturer's instruction.

RT-qPCR

For RT-qPCR, total RNA extractions were carried out on HKDM samples using RNAzol RT Isolation Reagent (Molecular Research Center, Cincinnati, OH, USA) in combination with the Pure Link RNA mini-kit (Invitrogen) that was used for DNAse treatment and washing steps only, following manufacturer protocols. Samples were resuspended in molecular-grade water (Ambion, TX, USA) and stored at –80°C until use. The RNA concentration and purity were determined using Nanodrop (BioTek Synergy LX Multi-Mode Reader, Daytona Beach, FL, USA) with software Gen5 version 3.11.

The qPCRs were carried out by qPCRBIO SyGreen 1-Step Go Lo-R kit (PCRBiosystems, Wayne, PA, USA). One-step qPCR was performed using 10 ng of respective RNA, 0.5 µM of each gene-specific primer (Table 1) in each reaction mixture under conditions of 54°C for 10 min, 95°C for 2 min, and 40 cycles of 95°C for 5 s and 61°C for 30 s in a LightCycler 96 System (Roche Applied Science, Indianapolis, IN, USA). Oligonucleotide primers were purchased from Integrated DNA Technologies (Coralville, IA, USA). The CanX was used as a reference gene.

Caspase activity

Cultures of HKDM infected with either wild-type *E. ictaluri* or ΔeseN were inoculated into three replicate wells (for each treatment) of a 24-well plate at an MOI of 10 bacteria per cell. Staurosporine (Sigma-Aldrich)-treated HKDMs (1 μM) were used as a positive control, and untreated HKDMs were used as a negative control. Caspase-8 and caspase-9 activity were measured using the Caspase-8/Caspase-9 Apoptosis Assay Kit (Cell Meter, Sunnyvale, CA, USA). Caspase-3/7 activity was measured using the Apo-ONE homogeneous caspase-3/7 assay (Promega, Madison, WI, USA). Cells in three wells of each treatment were lysed at 1, 3, and 5 h following caspase assay. Fluorescence was measured on a Spectra Max M2 microplate reader (Molecular Devices, Sunnyvale, CA, USA). Caspase activity was expressed as the ratio of infected to uninfected control cells (59).

Assessment of apoptosis by flow cytometry

Apoptosis was detected in HKDM infected with WT and Δ EseN strains of *E. ictaluri* using Alexa Fluor 647-labeled AnnV and Prl (Thermo Fisher, Waltham, MA, USA) according to the manufacturer's instructions. Uninfected HKDM and HKDM treated with 1- μ M staurosporine were used as controls. After 5 h of infection, macrophages were washed with PBS and removed from the six-well plate in 100 μ L of AnnV binding buffer. The cell suspension was then incubated with 5- μ L AnnV and 5 μ L of Pl in the dark for 15 min at room temperature. Finally, 400 μ L of binding buffer was added and the samples were analyzed within 1 h on a BD FACSCalibur cell analyzer (Becton, Dickinson and Company, Franklin Lakes, NJ, USA). A total of 50,000 cells were counted in each of the three replicated experiments. Samples were gated on the basis of forward versus side

TABLE 1 Primers used in this work for RT-qPCR

Primers	Forward (5′–3′)	Reverse (5'-3')	
CanX	GCT GTT AAA CCG GAG GAC TG	GCA GGT CCT CGA AGT AGT CAG	
apaf1	ACA TCG GCA TCC TGT ACG TC	GCC AGA AAC AGA TCG AAC GC	
p53	AGA CAG CCA GGA GTT TGC AG	AGT CCG GGG TAA TCG GAG GT	
BCL2	CGG CGG GAT CGT AAG AAG AT	TGA AAA CTG TCT GTC GCG GA	
Baxa	TCT GCG ACC CCA CCC ATA AA	CCA CCA CTC TGC CCC AGT TA	
IL-10	CTC CTC CCC CTG AGG ATT CA	CGG ATC ACG GCG TAT GAA GA	

scatter for size, and the results are presented as the percentage of cells that were viable (AnnV–/Prl–), early apoptotic (AnnV+/Prl–), or late apoptotic/necrotic (AnnV+/Prl+).

Anti-IL-1ß antibody preparation

The channel catfish IL-1 β gene was amplified from cDNA using a forward primer with sequence added to insert an *Ncol* site just upstream for cloning: CATGccatggATGGCT-GACGATTGTTAATGCTGAAA. The reverse primer contains an *Xhol* site: CCGGctcga-gATGGCTGACAAAGATTTGTTAATGCTG. The amplified fragment was cloned into the expression vector pET-26b and transferred into Nova Blue competent cells. Constructs were confirmed by plasmid isolation and DNA sequencing and subcloned into B21(DE3), and expression was induced with IPTG. Protein was purified using a HisPur Cobalt purification kit (Thermo Scientific).

The IL-1 β antibody was produced in a goat by injecting 1 mL of 1-mg/mL purified IL-1 β emulsified in Freund's complete adjuvant into each hind quadriceps five times at 2-week intervals. The titer of anti-EseN in the serum was determined by dot blot ELISA using purified IL-1 β . Specificity of anti-IL-1 β antibody was confirmed by Western blotting of whole serum and purified IL-1 β .

Immunoblotting

For immunoblotting, HKDMs were infected with WT, Δ EseN, or T3SS mutant for 5 h as described above. Medium was discarded and lysates from each of two replicate wells were collected using a cell scraper in 50 μ L of RIPA cell lysis buffer (Cell Signaling Technology) supplemented with PMSF (Thermo Scientific), Halt Protease Inhibitor Cocktail (Thermo Scientific), and PhosSTOP (Roche Diagnostic GmbH). Immediately after collection, lysates were added with 2× Laemmli Sample Buffer (Bio-Rad) supplemented with 2-mercaptoethanol (Sigma-Aldrich), aliquoted and stored at -80° C until use. Before loading in gel, samples were boiled for 5 min, separated by SDS-PAGE on 12% polyacrylamide gels (Bio-Rad) and transferred onto PVDF membranes (Bio-Rad). Membranes were blocked with 2% bovine serum albumin (Sigma-Aldrich) in Tris-buffered saline (Bio-Rad) with 0.2% Tween 20 (Sigma-Aldrich) for 1 h. The IL-1 β protein was detected with IL-1 β goat polyclonal antibody (this work). As a loading control, α/β -tubulin was detected using rabbit α/β -tubulin antibody (Cell Signaling Technology). Goat anti-rabbit IRDye 680RD and Donkey anti-goat IRDye 680RD (Li-COR) were used as secondary antibodies, followed by detection on a ChemiDoc MP imaging System (Bio-Rad).

TEM

The HKDMs were infected for 5 h as described above. Cells were washed with PBS and removed with a cell scraper. After centrifugation, at $500 \times g$, cells were fixed in 2% paraformaldehyde and 1.25% glutaraldehyde in 0.1-M cacodylate buffer with 5% sucrose for 1 to 2 h. The pellet was embedded in 3% agarose, cut into small cubes, washed in buffer, and post-fixed in 1% osmium tetroxide for 30 min–1 h. After rinsing in water, the samples were incubated in 2% uranyl acetate in sodium acetate buffer (pH 3.5) for 2 h, washed in water, dehydrated in a graded series of ethanol/propylene oxide, and embedded in epon-araldite. Thin sections were stained with uranyl acetate and lead citrate and examined in a JEOL JEM 1011 microscope. Samples for TEM were prepared and visualized at the Louisiana State University Electron Microscopy facility.

Cytotoxicity assay

Leakage of LDH from the cell cytoplasm as a measure of cytotoxicity was quantified using the CytoTox-ONE homogeneous cytotoxicity assay (Promega) at 3 and 5 h Pl. A spontaneous release control consisted of supernatant from non-infected HKDM. The maximum release control was the supernatant from cells lysed with 1% Triton X-100 for 1 min. Percentage cytotoxicity was calculated using the following formula: 100%

Microbiology Spectrum

Downloaded from https://journals.asm.org/journal/spectrum on 11 March 2024 by 2600:1700:a58:5270:1448:6640:10f7:5203.

× [(experimental release – spontaneous release)/(maximum release – spontaneous release)], as per the manufacturer's protocol.

Statistical analysis

All experiments were performed as three to five independent experiments. Statistical analysis of the data for the p38, JNK, and PDK1 inactivation was conducted by using one-way ANOVA followed by Tukey's post hoc test for comparison among treatments.

Each RT-qPCR assay was performed in technical triplicates, and relative expression was calculated by the normalized ratio obtained using LightCycler 96 Application Software. To improve this normalization step, CanX was chosen as reference gene. Results were further analyzed by using means from technical replicates of each sample. The relative ratio was calculated for each sample to detect differences between HKDM-WT and HKDM-EseN. Comparison between two groups was also analyzed by *t*-test. All statistical computations were performed with GraphPad Prism version 5.02 software (GraphPad Software).

ACKNOWLEDGMENTS

This research was supported by the National Science Foundation under grant no. 2100228.

AUTHOR AFFILIATIONS

¹Department of Biological Sciences and Chemistry, Southern University and A & M College, Baton Rouge, Louisiana, USA

²Department of Biology, University of Wisconsin-Stevens Point, Stevens Point, Wisconsin, USA

³Department of Pathobiological Sciences, Louisiana State University School of Veterinary Medicine, Baton Rouge, Louisiana, USA

PRESENT ADDRESS

Chanida Fongsaran, Department of Pathology, The University of Texas Medical Branch, Galveston, Texas, USA

AUTHOR ORCIDs

Lidiya Dubytska http://orcid.org/0000-0002-8949-7169

FUNDING

Funder	Grant(s)	Author(s)
National Science Foundation (NSF)	2100228	Lidiya Dubytska
		Ronald Thune

AUTHOR CONTRIBUTIONS

Ranjan Koirala, Data curation, Formal analysis, Methodology, Writing – review and editing | Chanida Fongsaran, Data curation, Methodology | Tanisha Poston, Data curation, Formal analysis | Matthew Rogge, Project administration, Writing – review and editing | Bryan Rogers, Writing – review and editing | Ronald Thune, Methodology, Project administration, Resources, Supervision, Writing – review and editing | Lidiya Dubytska, Conceptualization, Funding acquisition, Investigation, Methodology, Project administration, Resources, Supervision, Writing – review and editing

REFERENCES

- Coburn B, Sekirov I, Finlay BB. 2007. Type III secretion systems and disease. Clin Microbiol Rev 20:535–549. https://doi.org/10.1128/CMR.00013-07
- Thune RL, Fernandez DH, Benoit JL, Kelly-Smith M, Rogge ML, Booth NJ, Landry CA, Bologna RA. 2007. Signature-tagged mutagenesis of Edwardsiella ictaluri identifies virulence-related genes, including a Salmonella pathogenicity island 2 class of type III secretion systems. Appl Environ Microbiol 73:7934–7946. https://doi.org/10.1128/AEM.01115-07
- Dubytska LP, Thune RL. 2020. Early intracellular trafficking and subsequent activity of programmed cell death in channel catfish macrophages infected with *Edwardsiella ictaluri*. Microorganisms 8:1649. https://doi.org/10.3390/microorganisms8111649
- Dean P. 2011. Functional domains and motifs of bacterial type III effector proteins and their roles in infection. FEMS Microbiol Rev 35:1100–1125. https://doi.org/10.1111/j.1574-6976.2011.00271.x
- Baxt LA, Garza-Mayers AC, Goldberg MB. 2013. Bacterial subversion of host innate immune pathways. Science 340:697–701. https://doi.org/10. 1126/science.1235771
- Reddick LE, Alto NM. 2014. Bacteria fighting back: how pathogens target and subvert the host innate immune system. Mol Cell 54:321–328. https://doi.org/10.1016/j.molcel.2014.03.010
- Shan L, He P, Sheen J. 2007. Intercepting host MAPK signaling cascades by bacterial type III effectors. Cell Host Microbe 1:167–174. https://doi. org/10.1016/j.chom.2007.04.008
- Brennan DF, Barford D. 2009. Eliminylation: a post-translational modification catalyzed by phosphothreonine lyases. Trends Biochem Sci 34:108–114. https://doi.org/10.1016/j.tibs.2008.11.005
- Li H, Xu H, Zhou Y, Zhang J, Long C, Li S, Chen S, Zhou JM, Shao F. 2007. The phosphothreonine lyase activity of a bacterial type III effector family. Science 315:1000–1003. https://doi.org/10.1126/science.1138960
- Mittal R, Peak-Chew SY, McMahon HT. 2006. Acetylation of MEK2 and I kappa B kinase (IKK) activation loop residues by YopJ inhibits signaling. Proc Natl Acad Sci U S A 103:18574–18579. https://doi.org/10.1073/pnas. 0608995103
- Zhang J, Shao F, Li Y, Cui H, Chen L, Li H, Zou Y, Long C, Lan L, Chai J, Chen S, Tang X, Zhou JM. 2007. A *Pseudomonas syringae* effector inactivates MAPks to suppress PAMP-induced immunity in plants. Cell Host Microbe 1:175–185. https://doi.org/10.1016/j.chom.2007.03.006
- Neumann C, Fraiture M, Hernàndez-Reyes C, Akum FN, Virlogeux-Payant I, Chen Y, Pateyron S, Colcombet J, Kogel K-H, Hirt H, Brunner F, Schikora A. 2014. The Salmonella effector protein SpvC, a phosphothreonine lyase is functional in plant cells. Front Microbiol 5:548. https://doi.org/10.3389/fmicb.2014.00548
- Zurawski DV, Mitsuhata C, Mumy KL, McCormick BA, Maurelli AT. 2006.
 OspF and OspC1 are Shigella flexneri type III secretion system effectors that are required for postinvasion aspects of virulence. Infect Immun 74:5964–5976. https://doi.org/10.1128/IAI.00594-06
- Cargnello M, Roux PP. 2011. Activation and function of the MAPKs and their substrates, the MAPK-activated protein kinases. Microbiol Mol Biol Rev 75:50–83. https://doi.org/10.1128/MMBR.00031-10
- Chambers KA, Abularrage NS, Scheck RA. 2018. Selectivity within a family of bacterial phosphothreonine lyases. Biochemistry 57:3790– 3796. https://doi.org/10.1021/acs.biochem.8b00534
- Dubytska LP, Thune RL. 2018. Edwardsiella ictaluri type III secretion system (T3SS) effector EseN is a phosphothreonine lyase that inactivates ERK1/2. Dis Aquat Organ 130:117–129. https://doi.org/10.3354/ dao03255
- Dubytska LP, Koirala R, Sanchez A, Thune R. 2022. Edwardsiella ictaluri T3SS effector EseN modulates expression of host genes involved in the immune response. Microorganisms 10:1334. https://doi.org/10.3390/ microorganisms10071334
- Kolli S, Zito CI, Mossink MH, Wiemer EAC, Bennett AM. 2004. The major vault protein is a novel substrate for the tyrosine phosphatase SHP-2 and scaffold protein in epidermal growth factor signaling. J Biol Chem 279:29374–29385. https://doi.org/10.1074/jbc.M313955200
- Levina A, Fleming KD, Burke JE, Leonard TA. 2022. Activation of the essential kinase PDK1 by phosphoinositide-driven trans-autophosphorylation. Nat Commun 13:1874. https://doi.org/10.1038/s41467-022-29368-4

 Shakeri R, Kheirollahi A, Davoodi J. 2017. Apaf-1: regulation and function in cell death. Biochimie 135:111–125. https://doi.org/10.1016/j.biochi. 2017.02.001

- Molchadsky A, Rivlin N, Brosh R, Rotter V, Sarig R. 2010. p53 is balancing development, differentiation and de-differentiation to assure cancer prevention. Carcinogenesis 31:1501–1508. https://doi.org/10.1093/ carcin/bqq101
- Brady HJM, Gil-Gómez G. 1998. Bax. the pro-apoptotic Bcl-2 family member, Bax. Int J Biochem Cell Biol 30:647–650. https://doi.org/10. 1016/s1357-2725(98)00006-5
- Bzowska M, Guzik K, Barczyk K, Ernst M, Flad HD, Pryjma J. 2002. Increased IL-10 production during spontaneous apoptosis of monocytes. Eur J Immunol 32:2011–2020. https://doi.org/10.1002/1521-4141(200207)32:7<2011::AID-IMMU2011>3.0.CO;2-L
- Hazzalin CA, Le Panse R, Cano E, Mahadevan LC. 1998. Anisomycin selectively desensitizes signalling components involved in stress kinase activation and fos and jun induction. Mol Cell Biol 18:1844–1854. https:// doi.org/10.1128/MCB.18.4.1844
- Walker VG, Ammer A, Cao Z, Clump AC, Jiang B-H, Kelley LC, Weed SA, Zot H, Flynn DC. 2007. PI3K activation is required for PMA-directed activation of cSrc by AFAP-110. Am J Physiol Cell Physiol 293:C119–32. https://doi.org/10.1152/ajpcell.00525.2006
- Tzifi F, Economopoulou C, Gourgiotis D, Ardavanis A, Papageorgiou S, Scorilas A. 2012. The role of BCL2 family of apoptosis regulator proteins in acute and chronic leukemias. Adv Hematol 2012:524308. https://doi. org/10.1155/2012/524308
- Baumgartner WA, Dubytska L, Rogge ML, Mottram PJ, Thune RL. 2014.
 Modulation of vacuolar pH is required for replication of Edwardsiella ictaluri in channel catfish macrophages. Infect Immun 82:2329–2336. https://doi.org/10.1128/IAI.01616-13
- Ausubel FM. 2005. Are innate immune signaling pathways in plants and animals conserved? Nat Immunol 6:973–979. https://doi.org/10.1038/ ni1253
- Arbibe L, Kim DW, Batsche E, Pedron T, Mateescu B, Muchardt C, Parsot C, Sansonetti PJ. 2007. An injected bacterial effector targets chromatin access for transcription factor NF-kB to alter transcription of host genes involved in immune responses. Nat Immunol 8:47–56. https://doi.org/10. 1038/ni1423
- Bhavsar AP, Guttman JA, Finlay BB. 2007. Manipulation of host-cell pathways by bacterial pathogens. Nature 449:827–834. https://doi.org/ 10.1038/nature06247
- Diacovich L, Gorvel J-P. 2010. Bacterial manipulation of innate immunity to promote infection. Nat Rev Microbiol 8:117–128. https://doi.org/10. 1038/nrmicro2295
- Krzyzowska M, Swiatek W, Fijalkowska B, Niemialtowski M, Schollenberger A. 2014. The role of map kinases in immune response. Adv Cell Biol 2:125–138. https://doi.org/10.2478/v10052-010-0007-5
- 33. Zhang YL, Dong C. 2005. MAP kinases in immune responses. Cell Mol Immunol 2:20–27.
- Dubytska LP, Rogge ML, Thune RL. 2016. Identification and characterization of putative translocated effector proteins of the *Edwardsiella ictaluri* type III secretion system. mSphere 1:e00039-16. https://doi.org/10.1128/mSphere.00039-16
- Li Y, Yang KJ, Park J. 2010. Multiple implications of 3-phosphoinositidedependent protein kinase 1 in human cancer. World J Biol Chem 1:239– 247. https://doi.org/10.4331/wjbc.v1.i8.239
- Taniyama Y, Weber DS, Rocic P, Hilenski L, Akers ML, Park J, Hemmings BA, Alexander RW, Griendling KK. 2003. Pyk2- and Src-dependent tyrosine phosphorylation of PDK1 regulates focal adhesions. Mol Cell Biol 23:8019–8029. https://doi.org/10.1128/MCB.23.22.8019-8029.2003
- Schmutz C, Ahrné E, Kasper CA, Tschon T, Sorg I, Dreier RF, Schmidt A, Arrieumerlou C. 2013. Systems-level overview of host protein phosphorylation during Shigella flexneri infection revealed by phosphoproteomics. Mol Cell Proteomics 12:2952–2968. https://doi.org/10.1074/mcp.M113.029918
- Yue J, López JM. 2020. Understanding MAPK signaling pathways in apoptosis. Int J Mol Sci 21:2346. https://doi.org/10.3390/ijms21072346

 Wada T, Penninger JM. 2004. Mitogen-activated protein kinases in apoptosis regulation. Oncogene 23:2838–2849. https://doi.org/10.1038/sj.onc.1207556

- Zhang W, Liu HT. 2002. MAPK signal pathways in the regulation of cell proliferation in mammalian cells. Cell Res. 12:9–18. https://doi.org/10. 1038/si.cr.7290105
- Wada T, Stepniak E, Hui L, Leibbrandt A, Katada T, Nishina H, Wagner EF, Penninger JM. 2008. Antagonistic control of cell fates by JNK and p38– MAPK signaling. Cell Death Differ 15:89–93. https://doi.org/10.1038/sj. cdd.4402222
- Wagner EF, Nebreda AR. 2009. Signal integration by JNK and p38 MAPK pathways in cancer development. Nat Rev Cancer 9:537–549. https://doi. org/10.1038/nrc2694
- 43. Cuenda A, Rousseau S. 2007. p38 MAP-kinases pathway regulation, function and role in human diseases. Biochim Biophys Acta 1773:1358–1375. https://doi.org/10.1016/j.bbamcr.2007.03.010
- Zeke A, Misheva M, Reményi A, Bogoyevitch MA. 2016. JNK signaling: regulation and functions based on complex protein-protein partnerships. Microbiol Mol Biol Rev 80:793–835. https://doi.org/10.1128/ MMBR.00043-14
- 45. Dhanasekaran DN, Reddy EP. 2008. JNK signaling in apoptosis. Oncogene 27:6245–6251. https://doi.org/10.1038/onc.2008.301
- Fuchs SY, Adler V, Pincus MR, Ronai Z. 1998. MEKK1/JNK signaling stabilizes and activates p53. Proc Natl Acad Sci U S A 95:10541–10546. https://doi.org/10.1073/pnas.95.18.10541
- 47. Wolf ER, McAtarsney CP, Bredhold KE, Kline AM, Mayo LD. 2018. Mutant and wild-type p53 form complexes with p73 upon phosphorylation by the kinase JNK. Sci Signal 11:eaao4170. https://doi.org/10.1126/scisignal.aao4170
- Chen Y-F, Pandey S, Day CH, Chen Y-F, Jiang A-Z, Ho T-J, Chen R-J, Padma VV, Kuo W-W, Huang C-Y. 2018. Synergistic effect of HIF-1α and FoxO3a trigger cardiomyocyte apoptosis under hyperglycemic ischemia condition. J Cell Physiol 233:3660–3671. https://doi.org/10.1002/jcp. 26235
- McClelland Descalzo DL, Satoorian TS, Walker LM, Sparks NRL, Pulyanina PY, Zur Nieden NI. 2016. Glucose-induced oxidative stress reduces proliferation in embryonic stem cells via FOXO3A/β-catenin-dependent transcription of p21(cip1). Stem Cell Rep 7:55–68. https://doi.org/10. 1016/j.stemcr.2016.06.006
- McGowan SE, McCoy DM. 2013. Platelet-derived growth factor-A regulates lung fibroblast S-phase entry through p27(kip1) and FoxO3a. Respir Res 14:68. https://doi.org/10.1186/1465-9921-14-68

- Joseph J, Ametepe ES, Haribabu N, Agbayani G, Krishnan L, Blais A, Sad S.
 2016. Inhibition of ROS and upregulation of inflammatory cytokines by FoxO3a promotes survival against Salmonella Typhimurium. Nat Commun 7:12748. https://doi.org/10.1038/ncomms12748
- 52. Fluteau A, Ince PG, Minett T, Matthews FE, Brayne C, Garwood CJ, Ratcliffe LE, Morgan S, Heath PR, Shaw PJ, Wharton SB, Simpson JE, MRC Cognitive Function Ageing Neuropathology Study Group. 2015. The nuclear retention of transcription factor FOXO3a correlates with a DNA damage response and increased glutamine synthetase expression by astrocytes suggesting a neuroprotective role in the ageing brain. Neurosci Lett 609:11–17. https://doi.org/10.1016/j.neulet.2015.10.001
- Behar SM, Briken V. 2019. Apoptosis inhibition by intracellular bacteria and its consequence on host immunity. Curr Opin Immunol 60:103–110. https://doi.org/10.1016/j.coi.2019.05.007
- Sahoo M, Ceballos-Olvera I, del Barrio L, Re F. 2011. Role of the Inflammasome, IL-1β, and IL-18 in bacterial infections. Sci World J 11:2037–2050. https://doi.org/10.1100/2011/212680
- Ratner D, Orning MPA, Proulx MK, Wang D, Gavrilin MA, Wewers MD, Alnemri ES, Johnson PF, Lee B, Mecsas J, Kayagaki N, Goguen JD, Lien E. 2016. The Yersinia pestis effector YopM inhibits pyrin Inflammasome activation. PLoS Pathog 12:e1006035. https://doi.org/10.1371/journal. ppat.1006035
- Zwack EE, Snyder AG, Wynosky-Dolfi MA, Ruthel G, Philip NH, Marketon MM, Francis MS, Bliska JB, Brodsky IE. 2015. Inflammasome activation in response to the *Yersinia* type III secretion system requires hyperinjection of translocon proteins YopB and YopD. mBio 6:e02095-14. https://doi. org/10.1128/mBio.02095-14
- Booth NJ, Elkamel A, Thune RL. 2006. Intracellular replication of Edwardsiella ictaluri in channel catfish macrophages. J Aquat Anim Health 18:101–108. https://doi.org/10.1577/H05-025.1
- Shyu JF, Zhang Z, Hernandez-Lagunas L, Camerino C, Chen Y, Inoue D, Baron R, Horne WC. 1999. Protein kinase C antagonizes pertussis-toxinsensitive coupling of the calcitonin receptor to adenylyl cyclase. Eur J Biochem 262:95–101. https://doi.org/10.1046/j.1432-1327.1999.00346.x
- Zhao D, Lin F, Wu X, Zhao Q, Zhao B, Lin P, Zhang Y, Yu X. 2012. Pseudolaric acid B induces apoptosis via proteasome-mediated Bcl-2 degradation in hormone-refractory prostate cancer DU145 cells. Toxicol In Vitro 26:595–602. https://doi.org/10.1016/j.tiv.2012.02.004